Predictive modeling of thermoelastic energy dissipation in tunable MEMS mirrors

Houwen Tang
University of Denver
Department of Electrical and Computer Engineering
Denver, Colorado 80208

Yun-Bo Yi
University of Denver
Department of Mechanical and Materials Engineering
Denver, Colorado 80208
E-mail: yyi2@du.edu

Mohammad A. Matin
University of Denver
Department of Electrical and Computer Engineering
Denver, Colorado 80208

Abstract. The design of microstructures with a high quality factor (Q value) is of significant importance in many microelectromechanical system (MEMS) applications. Thermoelastic damping can cause an intrinsic energy loss that affects the Q value of high-frequency resonance in those devices such as MEMS mirrors. We deal with the simulation and analysis of thermoelastic damping of MEMS mirrors based on the finite element method. Four designs of MEMS mirrors with different geometric shapes are studied. In each model, the dynamic responses of the system subjected to thermoelastic damping are compared to those of the undamped modes. Then we present a systematic parametric study on both the resonant frequency and the Q value as functions of various representative parameters. These results are useful for early prediction of thermoelastic energy loss, not only restricted to the MEMS mirrors but also applicable in more general MEMS resonators and filters design.
 [DOI: 10.1117/1.2909274]

Subject terms: thermoelastic damping; MEMS mirror; finite element; quality factor.

Paper 07073R received Aug. 31, 2007; revised manuscript received Jan. 25, 2008; accepted for publication Feb. 11, 2008; published online Apr. 29, 2008.

1 Introduction

Microelectromechanical systems (MEMS) mirrors are widely used in modern high-tech industry, including high-speed Internet, wireless communication, biomedical system, and robots. For example, a MEMS mirror can be manufactured in the form of a tunable MEMS filter for dense wavelength-division-multiplexed (DWDM) optical networks,[1,2] as shown in Fig. 1. Techniques were developed to change the wavelength of a laser by tuning the cavity in the mirrors. In the design of these micromirror systems, energy consumption could be an important design consideration, especially for those applications involving wireless connections where the availability of power sources is limited. Therefore design of systems of low energy consumption is often a major concern. However, the dynamic deflection of microstructures connected to the mirrors under varying voltage can cause a structural resonance, which is associated with various damping mechanisms leading to energy dissipation. These mechanisms include (1) viscous effects,[3] (2) anchor losses,[4] (3) squeeze film damping,[5] and (4) the nonlinearity in the acoustic effects.[6] In addition to these mechanisms, it is strongly evident that thermoelastic damping, driven by the coupling between thermoelasticity and elastodynamics, is a dominant source of intrinsic damping in MEMS and nanoelectromechanical systems (NEMS) resonators operating at high frequencies.[7,8]

Briefly, thermoelastic damping occurs when a cyclic stress is applied to a material and the stress leads to an oscillatory deformation of the structure.[9] The energy is lost irreversibly when the heat flows from the compressed part (hot region) to the stretched part (cold region) in the material. The lost energy can be evaluated by the measure of the quality factor, a factor that compares the time constant for decay of an oscillating system's amplitude to its oscillation period. Physically speaking, the Q value is 2π times the ratio of the total energy stored divided by the energy lost in a single cycle. Equivalently, it compares the frequency at which a system oscillates to the rate at which it dissipates its energy.

The theory of thermoelastic damping was first established by Zener[10] who developed a general theory for thin beams in bending. However, Zener's derivation involved some mathematical and physical simplifications. Lifshitz and Roukes[11] successfully removed these simplifications, and derived an exact expression of the solution from the fundamental theories of thermoelasticity and elastodynamics. The same technique was later extended to other problems involving microplates of finite width[12] as well as in-plane vibration of MEMS gyros.[13,14] In addition, Sun et al.[15] studied thermoelastic damping in beam resonators under a variety of boundary conditions using a special technique called "the finite sine Fourier transformation method." Recently, a research group also reported some results regarding the link between Zener's analytical solution for a simple reed in bending and the solutions of more complicated resonator shapes.[16,17] Among all the numerical methods used to solve the problem of interest, the finite element discretization scheme has been shown to be the most successful one to date. For example, Silver and Peterson[18] used a differential stiffness matrix to solve the thermoelastic damping problem for beams. Yi and Martin[19] and Yi[20] developed a generalized eigenvalue scheme in conjunction with the finite element method to solve the problem in an arbitrary 2-D or 3-D domain, although some earlier works already existed in the literature, e.g., Gorman.[21] In fact, the finite element formulation for solv-

1537-1646/2008/$25.00 © 2008 SPIE

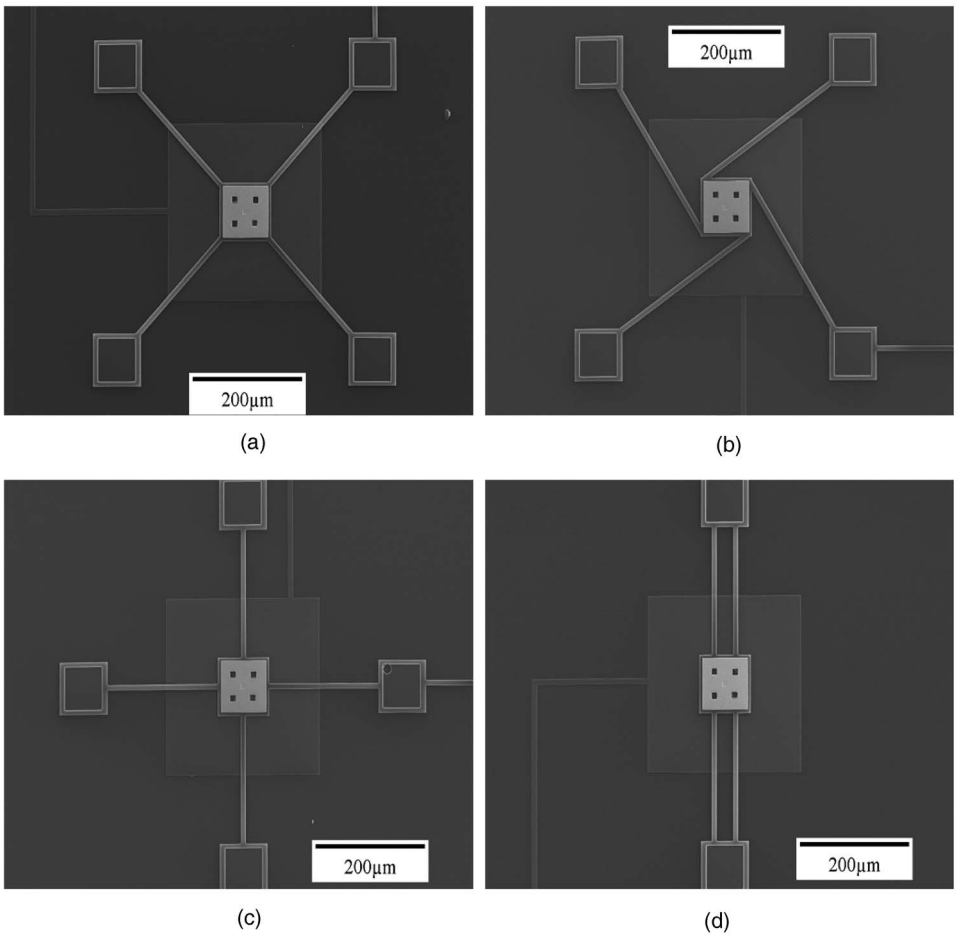

Fig. 1 Scanning electron microscopy (SEM) images of the existing micromirror designs. The scale bar is 200 μm.

ing the thermoelastic damping problems has successfully been implemented in several widely used commercial packages including COMSOL® and ANSYS®.

In this paper, we show the application of the COMSOL® software to solve the thermoelastic damping induced energy dissipation problem in MEMS mirrors for four distinct designs. Analytical approaches would otherwise be difficult to implement in the current problem due to the 3-D geometry and the complex boundary conditions involved. Parametric analyses are performed to investigate the effects of design parameters on the resonant frequency and Q value. Since a higher Q indicates a lower rate of energy dissipation relative to the oscillation frequency, and a lower Q indicates a greater rate of energy loss leading to the reduction of the sensitivity and more power consumption, we target minimizing the energy loss and therefore optimizing the design for maximum Q value in the current research. In addition, the computational accuracy is among the major concerns because without an accurate prediction tool the optimal structure would not be identified among the existing or proposed design schemes.

2 Methods

For a simply supported beam structure, analytical expressions were developed by prior researchers to estimate the thermoelastic damping energy dissipation. According to Zener,[9,10] the Q value can be calculated with a single thermal mode by

$$\frac{1}{Q} = \left(\frac{E\alpha^2 T_0}{\rho C_p}\right)\left[\frac{\omega\tau}{1+(\omega\tau)^2}\right], \tag{1}$$

where E is Young's modulus, α is the thermal expansion coefficient, T_0 is the resonator's mean temperature at rest, ρ is the density, C_p is the heat capacity of the material, ω is the resonant frequency, and τ is the thermal relaxation time of the system. From this equation, it can be seen that to obtain a high quality factor, the system must be designed in such a way that ω is as far from $1/\tau$ as possible.

The natural frequency of an undamped, simply supported beam system[22] can be calculated by

$$\omega_0 = \frac{\pi^2 h}{L^2}\left(\frac{E}{12\rho}\right)^{1/2}, \tag{2}$$

where L and h are the length and the thickness of the beam, respectively; E is Young's modulus; and ρ is the density. The thermal relaxation time of a beam[11] is given by

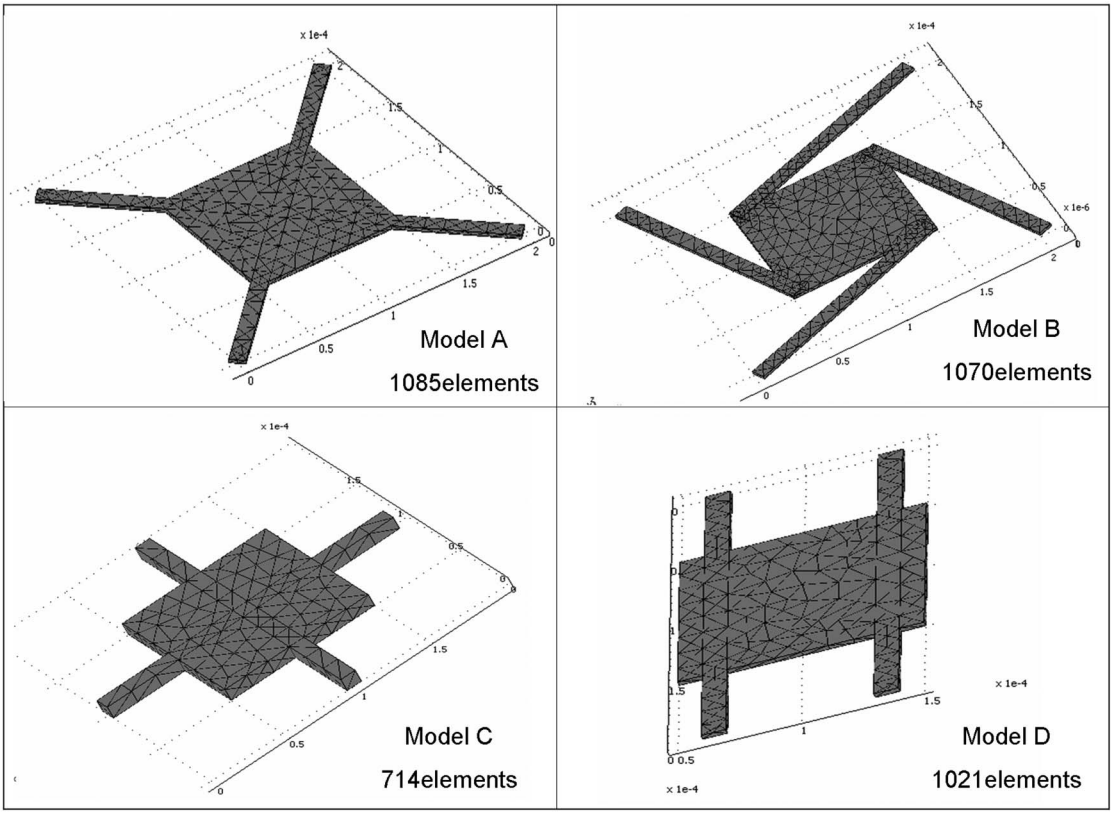

Fig. 2 Finite element models of the four different MEMS mirror designs shown in Fig. 1.

$$\tau = \frac{\rho C_p h^2}{\pi^2 k} \tag{3}$$

where k is the thermal conductivity. The preceding equations are applicable only to a simply supported beam structure. For more complex structures and boundary conditions, such as are involved in the MEMS mirror applications, a generalized eigenfrequency analysis is required to determine the dynamic characteristics of the system. Particularly, the variables in the governing differential equations are expressed in a perturbation form with an exponential decay rate. Time is canceled in the resulting equations, leading to an eigenvalue equation. The eigenvalue λ of either a damped or an undamped system contains the information about both the resonant frequency ω and the Q value. Here λ appears to be a complex value, and one can relate λ to ω and Q according to the following equations:

$$\omega_0 = |\text{img}\ (\lambda)|, \tag{4}$$

$$Q = \left| \frac{\text{img}\ (\lambda)}{2\ \text{real}\ (\lambda)} \right|, \tag{5}$$

where img(λ) and real(λ) are the imaginary part and real part of λ, respectively. In COMSOL®, the preceding eigenvalue scheme is integrated into the finite element formulation. Therefore, this capability was directly incorporated in our study. The construction of the MEMS mirror computational model using COMSOL® follows a procedure described in the following. First, the 3-D beam and mirror geometries were created individually and then merged together by applying the appropriate Boolean operations. The interior boundaries were then deleted. An external code was implemented to enable the changes of the geometric properties required in the parametric analyses. Second, the finite element mesh consisting of tetrahedron elements was generated using the built-in mesh generation functions, as shown in Fig. 2. The local mesh density and element size were controllable through a set of meshing parameters. Finally, the governing differential equation for heat conduc-

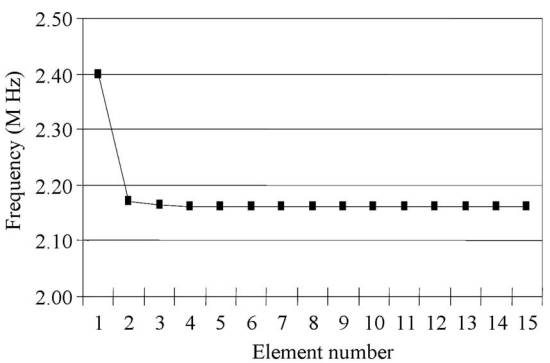

Fig. 3 Convergence test showing the relationship between the resonant frequency and the finite element number for the first undamped modes of a simply supported beam.

Table 1 Polysilicon material properties.

Young's modulus, (E) (Pa)	1.61×10^{11}
Poisson's ration	0.22
Thermal expansion coefficient, α (K^{-1})	2.6×10^{-6}
Thermal conductivity, K ($W\ m^{-1}\ K^{-1}$)	34
Specific heat ($m^2\ s^{-1}$)	678
Density, ρ (kg/m^3)	2320
Temperature (K)	300

Table 2 Dominant mode frequencies.

	Model A	Model B	Model C	Model D
Mode 1 (MHz)	0.202	0.092	2.43	0.295
Mode 2 (MHz)	0.533	0.210	4.87	0.473
Mode 3 (MHz)	0.536	0.210	4.98	0.884
Mode 4 (MHz)	1.130	0.719	5.82	1.44
Mode 5 (MHz)	1.780	0.925	6.96	1.86

tion involving thermoelastic damping as follows was specified in the model description portion as required by the COMSOL® package.

$$k\nabla^2 T = \rho C_p \frac{\partial T}{\partial t} + \frac{E\alpha T_0}{1-2\nu}\frac{\partial(\varepsilon_x+\varepsilon_y+\varepsilon_z)}{\partial t}, \tag{6}$$

where ε_x, ε_y, and ε_z are the strains in the x, y, and z directions, respectively; and ν is Poisson's ratio.

3 Numerical Results

3.1 *Convergence Analyses*

We first performed a parametric analysis on the effect of the element number on the accuracy of the beam results. The commercial finite element code Abaqus CAE® was used in this analysis. A simply supported beam was divided into a number of finite elements in the longitudinal direction and the natural frequency of resonance was computed using a generalized eigenfrequency scheme. The beam size used was $0.1\times0.1\times1$ μm. The computational result is shown in Fig. 3. Apparently, it can be seen that the resonant frequency becomes asymptotic when the element number increases. In comparison to the theoretical solution of the undamped resonant frequency, the finite element results are sufficiently accurate when the element number is greater than about 10. However, an element number less than 5 could result in an appreciable inaccuracy in the solution. In practice, 10 elements along the length should be considered as the minimum requirement for the beam problem under investigation. On the other hand, too many elements will make the computation cumbersome and should be avoided.

Four distinct MEMS mirror designs shown in Figs. 1 and 2 were then analyzed and compared. The material used for both the mirrors and the beams are polysilicon, which has widely been used in the manufacturing of surface-micromachined devices.[23] See Table 1 for polysilicon material properties. For each of the four designs, multiple resonant modes could be excited and the different modes correspond to different resonant frequencies as well as Q values (as shown in Table 2). Not all of the modes, however, are important in engineering practice (e.g, some higher order modes are difficult to excite in real applications). In this paper, we focus on the first dominant mode (namely, the mode of the lowest resonant frequency) only. The information for higher order modes can be inferred from the results of the first mode.

In all the four models, the peripheral beams connected to the central mirror are assumed to be fixed at the end; the mirror in the middle is free to vibrate. Both the beams and the mirror have the same thickness. The entire device is considered to be thermally insulated and the initial temperature is set to 300 K.

3.2 *Resonant Frequency*

In this part of the study, we first investigated the effect of the mirror size on the resonant frequency. From the results

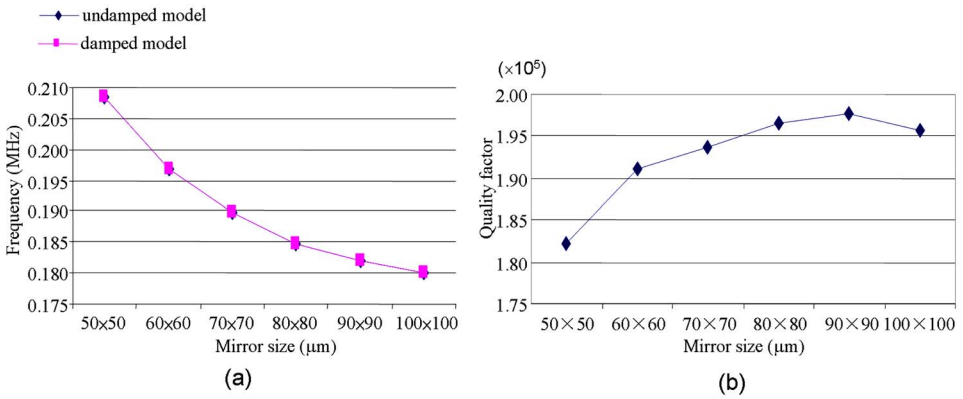

Fig. 4 (a) Frequency and (b) quality factor as functions of the mirror size in model A.

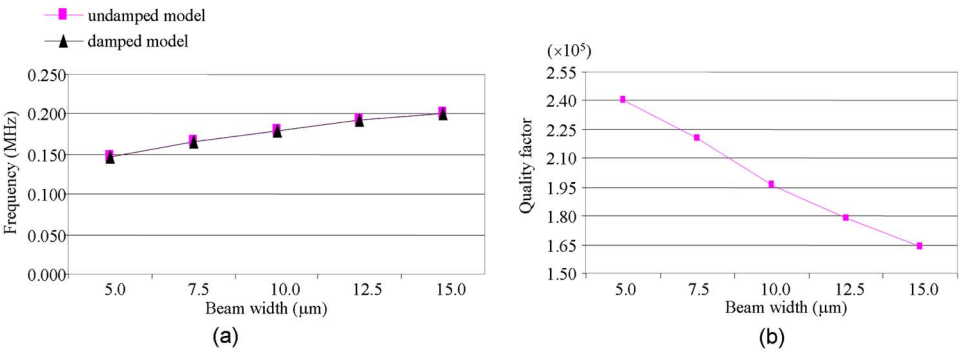

Fig. 5 (a) Frequency and (b) quality factor as functions of the beam width in model A.

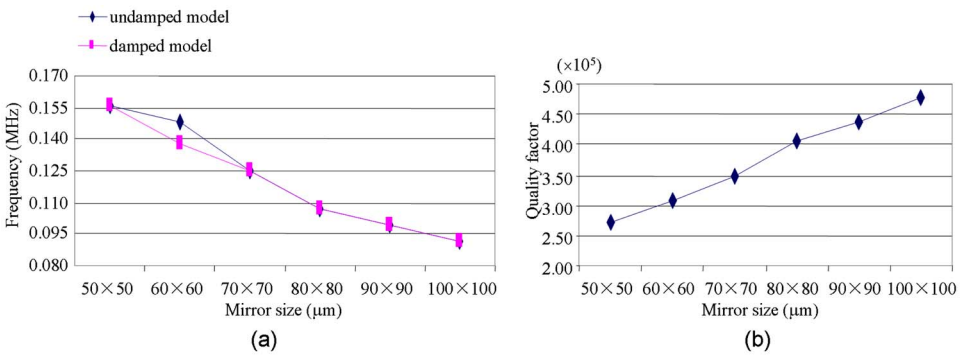

Fig. 6 (a) Frequency and (b) quality factor as functions of the mirror size in model B.

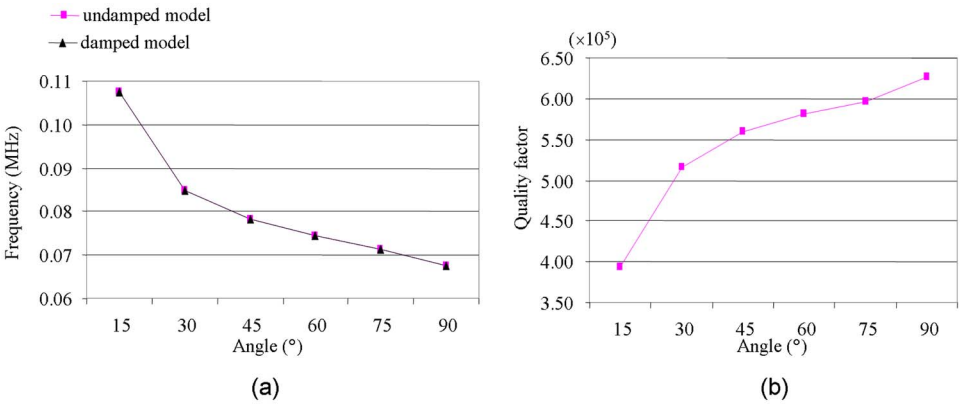

Fig. 7 (a) Frequency and (b) quality factor as functions of the angle between two adjacent beams in model B.

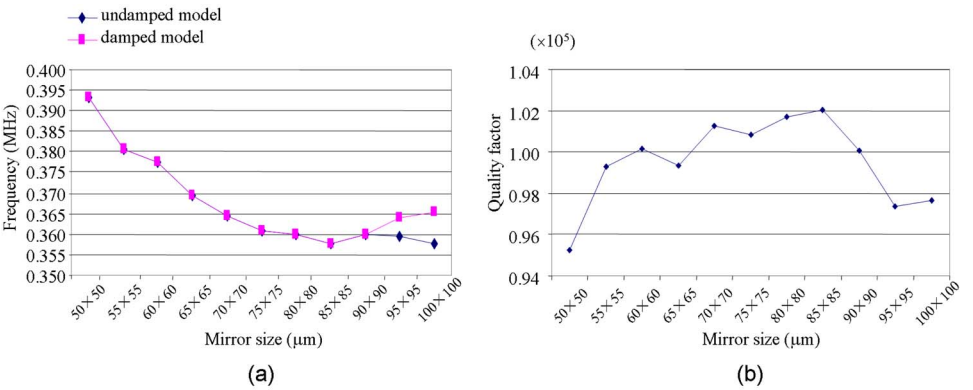

Fig. 8 (a) Frequency and (b) quality factor as functions of the mirror size in model C.

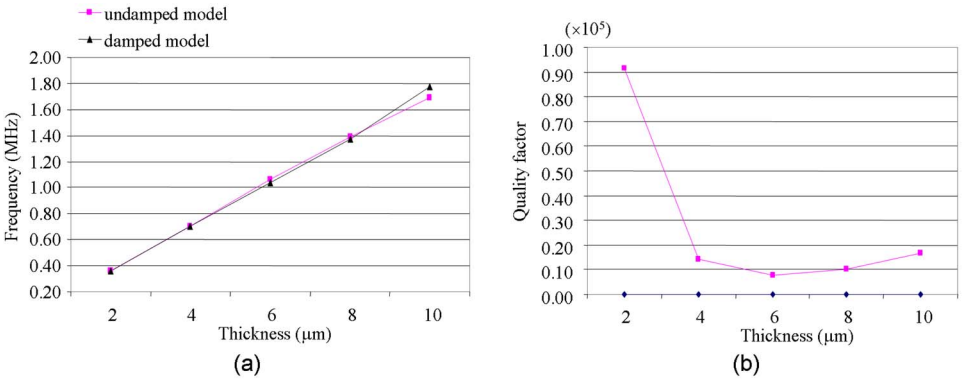

Fig. 9 (a) Frequency and (b) quality factor as functions of the beam thickness in model C.

shown in Fig. 4(a) we found that the resonant frequencies in the presence of thermoelastic damping for all the models were close to the frequencies of the undamped modes. The results also show that the frequency drops when the mirror size increases. This is because the device can be approximated as an equivalent spring-mass system in which the mass increases with the mirror size. Although the equivalent spring constant also changes with the mirror size at the same time, the effect of the mass will dominate, leading to a lower resonant frequency.

In addition to the mirror size, several other geometric factors were taken into consideration. One of these is the beam width. In this study, we used model A to investigate the relationship between the beam width and the eigenfrequency of the model. The result in Fig. 5(a) shows that the eigenfrequency increases with the beam width. This can be explained again by considering the entire device as an equivalent spring-mass system. An increase of the beam width will increase the equivalent spring constant, and therefore raise the resonant frequency. In view of this, the MEMS mirror should be designed in a way such that the beam width is sufficiently large to avoid any possible structural resonance with external vibrations.

Model B is a design with four beams connected to the corners of the central mirror at an inclined angle. The results in Fig. 6(a) show that the frequency decreases with the mirror size. We also investigated the frequency as a function of the included angle between the beam and the mirror. Figure 7(a) shows that the frequency decreases with the angle. It can be explained as follows. When the angle increases, the distance between the equivalent mass center and the fixed point of the beam increases and makes the spring system more flexible. This will result in a reduced spring constant and therefore the resonant frequency is raised.

We next investigated model C. Again, the resonant frequency decreases with the mirror size, as shown in Fig. 8(a). The impact of the beam thickness is shown in Fig. 9(a), from which we can see that the frequency changes with the beam thickness nearly along a straight line. This is consistent with the fundamental beam theory, in which the predicted frequency is linearly dependent on the beam thickness.

In model D, compared to the preceding results there is nothing unusual for the relationship between the frequency and the mirror size [Fig. 10(a)]. However, Fig. 11(a) shows that the resonant frequency increases with the beam spacing, although this change is much smaller than the changes caused by other factors. In fact, for both damped and undamped models, the maximum change in the resonant frequency is less than 5%.

3.3 *Quality Factor*

Quality factor is a major measurement to the energy dissipation. In fact, the magnitude of the energy loss largely

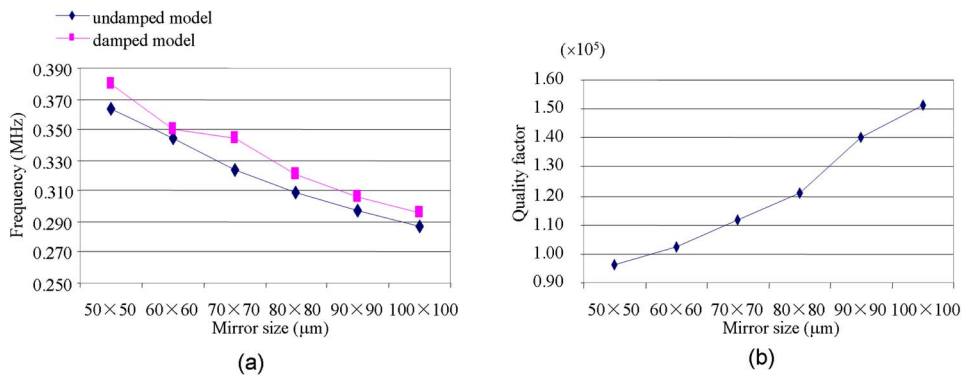

Fig. 10 (a) Frequency and (b) quality factor as functions of the mirror size in model D.

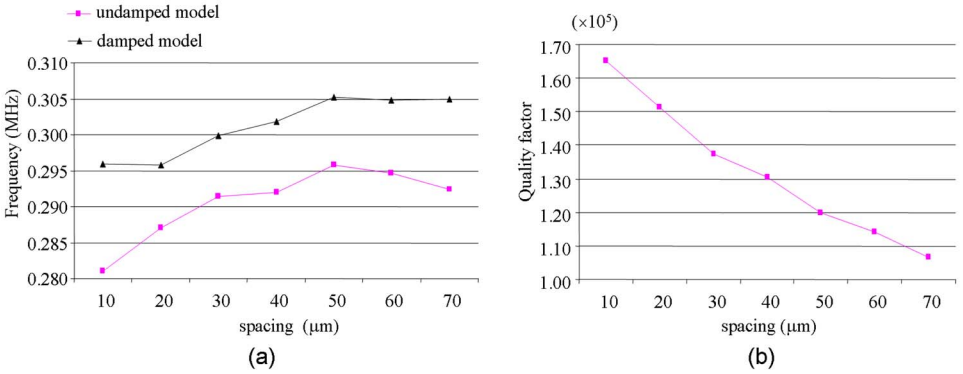

Fig. 11 (a) Frequency and (b) quality factor as functions of the beam spacing in model D.

relies on two factors, which are the resonant frequency and the structure's thermal relaxation time constant. The thermal relaxation time constant is the effective time that the material requires to relax after an applied constant stress or strain. Therefore, the effect of thermoelastic dissipation, which consequently leads to the damping is most pronounced when the vibration frequency is close to the thermal relaxation frequency. The impact of geometric changes on the Q value was studied for all four models.

In our study, we applied different mirror sizes in each model to compute the quality factor. Among all the mirror sizes being investigated for model A [Fig. 4(b)], it was found that the $90\times90\times2$ μm mirror size has the largest quality factor (1.98×10^5) among all the variable geometries. This means that this mirror size has the least energy loss induced by thermoelastic damping. Comparing the quality factor to the resonant frequency reveals that there is not a monotonic relationship between the quality factor and the frequency. In fact, when the real part of the eigenfrequency decreases, the imaginary part of the eigenfrequency could decrease more rapidly than the real part, which leads to an increase of the quality factor. The quality factors of models B and D increase with the mirror size, as shown in Figs. 6(b) and 10(b). By comparing the quality factor of model B with other models of the same parameters, it is easy to determine that model B has the largest quality factor. In fact, model B with a mirror size of $100\times100\times2$ μm has the higher Q value ($\sim4.8\times10^5$) among all the four designs A through D. For model C, the quality factor does not exhibit linear changes [Fig. 8(b)]. Among all the results obtained for model C, the quality factor corresponding to the mirror size $85\times85\times2$ μm is the greatest. However, this value is much smaller than for model A or model B.

In model A, the Q value was obtained by varying the beam width. According to the results, it has been found that the mirror with a wide beam has a much smaller Q value than the one with a narrow beam [as shown in Fig. 5(b)]. This is consistent with the results reported in the literature showing that the quality factor decreases with the elastic modulus. In model B, the included angle between the beam and the mirror was varied in the analysis and the significant changes in the quality factor can be seen in Fig. 7(b). The Q value reaches the highest point when the angle is 90 deg. In model C, the effect of the beam thickness was investigated. The quality factor has a relatively large value when the device is thin, and the value decreases rapidly when the thickness is increased [as shown in Fig. 9(b)]. On the other hand, in model D, the quality factor decreases when the spacing between two adjacent beams is increased [as shown in Fig. 11(b)]. Again these results can be explained by approximating the device as an equivalent single beam system and they are consistent with both the analytical[11] and numerical results[19] reported in the literature.

4 Conclusions

A set of parametric analyses was performed to systematically investigate the energy dissipation induced by thermoelastic damping in MEMS mirrors. The impact of different design schemes was studied. Because of the geometric complexity of the MEMS mirrors, the finite element method was applied. Based on the numerical results obtained from the four distinct designs, it was found that the resonant frequencies of the damped and undamped modes are generally very close. An increase in the central mirror size will lead to a decrease in the resonant frequency, whereas the quality factor typically increases. On the other hand, an increase of the thickness of the entire structure will lead to a higher resonant frequency yet a lower quality factor. The beam section also plays an essential role: increasing the beam width leads to higher frequency, but a lower quality factor.

From the standpoint of minimizing energy loss due to thermoelastic damping, model B with a mirror size of $100\times100\times2$ μm and an included angle of 90 deg between the peripheral beam and the central mirror exhibits the highest Q value and is therefore the best design among the four models being investigated. However, in practice, various factors may be considered simultaneously: for example, the optimization of the configuration with the greatest deflection range might have a higher priority than the consideration of energy consumption.

The techniques used in this paper can be readily extended to solve thermoelastic damping problems involved in more complex geometries. However, the computational time increases considerably with the degrees of freedom, especially when the damping is coupled with other physical processes such as electrostatic deformation. The develop-

ment of reduced-order models, which is part of our future work, is therefore essential to enhance the numerical efficiency in the computation.

References

1. Y. Guan and M. A. Matin, "Design and analysis of MEM-micromirrors for vertical cavity surface emitting lasers," *Microwave Opt. Technol. Lett.* **37**, 410–413 (2003).
2. Y. Guan and M. A. Matin, "Dynamic behavior of MEM-mirrors for tunable-VCSELs," *Microwave Opt. Technol. Lett.* **39**, 203–207 (2003).
3. D. Homentcovschi and R. N. Miles, "Viscous damping of perforated planar micromechanical structures," *Sens. Actuators, A* **119**, 544–552 (2005).
4. Y. H. Park and K. C. Park, "High-fidelity Modeling of MEMS resonators - Part 1: Anchor loss mechanisms through substrate," *J. Microelectromech. Syst.* **13**, 238–247 (2004).
5. P. Y. Kwok, M. S. Weinberg, and K. S. Breuer, "Fluid effects in vibrating micromachined structures," *J. Microelectromech. Syst.* **14**, 770–781 (2005).
6. R. Vinokur, "Vibroacoustic effects in MEMS," *Sound Vib.* **37**, 22–26 (2003).
7. T. V. Roszhart, "The effect of thermoelastic internal friction on the *Q* of micromachined silicon resonators," in *Proceeding IEEE Solid-State Sensors Actuator Workshop, 4th Technical Digest*, pp. 13–16, IEEE, Hilton Head, SC (1990).
8. S. Evoy, A. Olkhovets, L. Sekaric, J. M. Parpia, H. G. Craighead, and D. W. Carr, "Temperature-dependent internal friction in silicon nanoelectromechanical systems," *Appl. Phys. Lett.* **77**, 2397–2399 (2000).
9. C. Zener, "Internal friction in solids I: theory of internal friction in reeds," *Phys. Rev.* **52**, 230–235 (1937).
10. C. Zener, *Elasticity and Anelasticity of Metals*, the University of Chicago Press, Chicago (1948).
11. R. Lifshitz and M. L. Roukes, "Thermoelastic damping in micro- and nanomechanical systems," *Phys. Rev. B* **61**, 5600–5609 (2000).
12. A. H. Nayfeh and M. I. Younis, "Modeling and simulations of thermoelastic damping in microplates," *J. Micromech. Microeng.* **14**, 1711–1717 (2004).
13. S. J. Wong, C. H. J. Fox, and S. McWilliam, "Thermoelastic damping of the in-plane vibration of thin silicon rings," *J. Sound Vib.* **293**, 266–285 (2006).
14. A. Duwel, J. Gorman, M. Weinstein, J. Borenstein, and P. Ward, "Experimental study of thermoelastic damping in MEMS gyros," *Sens. Actuators, A* **103**, 70–75 (2003).
15. Y. Sun, D. Fang, and A. K. Soh, "Thermoelastic damping in microbeam resonators," *Int. J. Solids Struct.* **43**, 3213–3229 (2006).
16. B. H. Houston, D. M. Photiadis, M. H. Marcus, J. A. Bucaro, X. Liu, and J. F. Vignola, "Thermoelastic loss in microscale oscillators," *Appl. Phys. Lett.* **80**, 1300–1302 (2002).
17. X. Liu, J. F. Vignola, H. J. Simpson, B. R. Lemon, B. H. Houston, and D. M. Photiadis, "A loss mechanism study of a very high *Q* silicon micromechanical oscillator," *J. Appl. Phys.* **97**, 023524 (2005).
18. M. J. Silver and L. D. Peterson, "Predictive elastothermodynamic damping in finite element models by using a perturbation formulation," *AIAA J.* **43**, 2646–2653 (2005).
19. Y. B. Yi and M. A. Matin, "Eigenvalue solution of thermoelastic damping in beam resonators using a finite element analysis," *ASME J. Vibr. Acoust.* **129**, 478–483 (2007).
20. Y. B. Yi, "Geometric effects on thermoelastic damping in MEMS resonators," *J. Sound Vib.* **309**, 588–599 (2008).
21. J. P. Gorman, "Finite element analysis of thermoelastic damping in MEMS," MS Thesis, Massachusetts Institute of Technology, Department of Materials Science and Engineering (2002).
22. W. T. Thomson and M. D. Dahleh, *Theory of Vibration with Applications*, 5th ed., Prentice Hall, Upper Saddle River, NJ (1997).
23. R. Abdolvand, H. Johari, G. K. Ho, A. Erbil, and F. Ayazi, "Quality factor in trench-refilled polysilicon beam resonators," *J. Microelectromech. Syst.* **15**, 471–478 (2006).

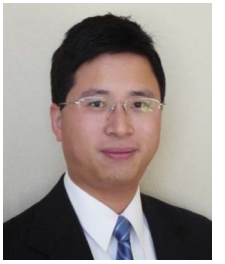

Yun-Bo Yi received his PhD degree in mechanical engineering in 2001 from the University of Michigan, Ann Arbor, where after 2 years of postdoctoral research work, he was promoted to assistant research scientist. In 2005 he sought a professorial job and later joined the faculty at the University of Denver. He received his MS degree from the University of Missouri, Rolla, in 1997 and his BS degree in automotive engineering from Tsinghua University, China, in 1994. Before he came to the United States, he was with the Shanghai Automotive Research Institute for nearly 1 year.

Biographies and photographs of the other authors not available.